PRIMARY PRODUCTION IN THE COASTAL ZONE

TABLE OF CONTENTS

Page:

List of Tables

List of Figures

Assignment

Topic

"What is the relationship between nutrient flux and primary production in the coastal zone? (What are some of the physical oceanographic processes controlling nutrient flux?")

Assigned Reading

Eppley, R. W., E. H. Renger, and W. G. Harrison.1979. Nitrate and phytoplankton production in southern California coastal waters. Limnol. Oceanogr. *24*: 483-494.

Riley, G. A. 1967. Mathematical model of nutrient conditions in coastal waters. Bull. Bingham Oceanogr. Coll. *19*: 72-80.

SUPPLEMENTAL

Ryther, J. H. and W. M. Dunstan 1971. Nitrogen, phosphorus and eutrophication in the coastal environment. Science *171*: 1008-1013.

Bruland, K. W., E. L. Rue, and G. J. Smith. 2001. Iron and macronutrients in California upwelling regimes: implications for diatom blooms. Limnol. Oceanogr. *46*: 1661-1674 *[Monterey Bay and north is Fe-replete, and large diatom blooms result. South of Monterey, in the Big Sur regions, Fe is depleted (< 1 nM), indicative of HNLC systems. See also **Hutchins & Bruland 1998**]*

Some Comments on the Assigned Reading

Riley (1967) describes a simple, but insightful, box model of neritic production. When reading this paper, you might consider how much of the offshore gradient in dissolved inorganic nitrogen (DIN) concentration, phytoplankton standing stock and production in MA Bay is due to the input from Boston Harbor's sewage outfalls. These gradients were documented in Parker's (1975) Ph.D. dissertation, and are now being documented by the MWRA. An alternate hypothesis would be that the production is driven by an inshore horizontal nutrient flux from the larger Gulf of Maine bottom waters driven by increased nearshore vertical mixing.

Riley (1967) should not be regarded as the definitive, nor even the accepted description of nutrient dynamics on continental shelves. **Ryther & Dunstan (1971)** describe the central importance of New York's sewer outfalls on New York bight nutrient dynamics. In stratified estuaries, the shore-ward transport of nutrient-rich bottom water can be driven by thermohaline (*i.e.*, estuarine) advective circulation, rather than simply by differential vertical diffusion.

Eppley *et al.* (1979) describe a variety of approaches used to refute three null hypotheses, framed to test the importance of nitrogen limitation in California shelf waters. They based their **null** hypotheses on the proposition that phytoplankton growth is independent of nitrate flux. Before discounting the importance of **Eppley *et al.* (1979)** as merely the rather elaborate refutation of a null hypothesis that everyone knows is false, consider the following section from **Harris's (1986)** Physiological Phytoplankton Ecology:

> *"Direct evidence for N limitation of growth rates in the oceans is hard to find. In the oceans, evidence which points to high production and a lack of N limitation has been obtained from a number of sources. Interestingly, none of these pieces of data (except Riley 1951) comes from the usual bottle techniques..." (p. 141)*
> *"The substitution of opportunist species should occur in all water types and hence the relative growth rates of phytoplankton should be close to the maximal values in all water types, even the most oligotrophic....As critical nutrient elements become scarce in surface waters during the period of summer stratification the whole planktonic community is driven to rapid nutrient*

> *regeneration and rapid recycling rates and there is a change in the species composition of the phytoplankton. Maximum relative growth rates are maintained....both N and P limitation occur rarely in both marine and freshwater. The received version of phytoplankton ecology is not borne out by this data...The response to nutrient depletion is a community response, and the only time that severe nutrient depletion and a reduction in growth should be observed is when a single-species bloom occurs." (p. 154)*

Harris's controversial views are consistent with Goldman's (**Goldman *et al.*1979**, **Goldman 1980**) arguments that most phytoplankton in the sea are growing at or near μ_{max}. That is, their relative growth rate approaches unity.

Definition of terms and concepts

Modus tollens and the role of the null hypothesis in ecology.
Advection-diffusion (=Fokker-Planck) equation.
A=dynamic eddy viscosity [g cm^{-1} s^{-1}]
Shear stress:

$$\tau_{xz} = A_z \frac{dU}{dz}.$$

where, A_z = *Dynamic eddy diffusivity.*
$\frac{d}{dz}$ = *first derivative, z-direction.*
τ_{xz} = *shear stress.*
U = *Water velocity, x-direction.*
Dimensions:

$$\left[\frac{g}{cm\ s^{-2}}\right] = \left[\frac{g}{cm\ s}\right]\left[\frac{cm\ s^{-1}}{cm}\right].$$

New vs. regenerated production (Eppley, p. 484 lower right)
New production: production that can be directly coupled to nitrate
How is ρ_{NO3^-} measured (Answer mass spectrometry)

Kinematic Eddy diffusion Coefficients (K_z's)

Mixing processes in both the water and sediments are modeled using the advection-diffusion equation:

$$\frac{dC}{dt} = \frac{\partial C}{\partial t} + u\frac{\partial C}{\partial x} + v\frac{\partial C}{\partial y} + w\frac{\partial C}{\partial z} \approx K_x\frac{\partial^2 C}{\partial x^2} + K_y\frac{\partial^2 C}{\partial y^2} + K_z\frac{\partial^2 C}{\partial z^2} + R, \qquad (2)$$

The K_x, K_y, and K_z parameters are the kinematic diffusivities (see Appendix I - terms for a description of the terms in this equation). **Table 1** provides a listing of the values of the kinematic diffusion coefficients from a variety of environments. Most of these values are modeled estimates. For comparative purposes, **Table 1** also shows the values for the molecular diffusion coefficients for O_2 and CO_2 (these are functions of temperature).

Table 1. Kinematic eddy diffusion coefficients from the literature

Medium	x or z	Depth	Location	Value $cm^2\ s^{-1}$	Reference/ Comments
Water	Horizontal	Surface	New England Coast	2.9×10^6	**Riley (1967)** Assumed
		Surface	S. California Bight	10^6	**Eppley *et al.* (1979)** Assumed
	Vertical	Surface Mixed Layer	S. California Bight	0.8-4	**Eppley *et al.* (1979)** Estimated from NO_3^- flux
		Above pycnocline	Sargasso Sea	2.3	**Altabet (1989, p. 1197)**
Water	Vertical	Pycnocline	Worldwide	1	Munk, quoted in **Lewis *et al.* 1986**
Water	Vertical	Pycnocline	Worldwide	0.2 - 0.75	**King & Devol (1979)** quoting Broecker 1966 (Based on radiotracers
Water	Vertical	Pycnocline	Eastern Tropical Pacific	0.05 - 1.1	**King & Devol (1979)**, using ^{15}N-uptake, as in Eppley and heat flux
Water	Vertical	Pycnocline	Oligotrophic Atlantic	.1 - .8 (& some lower)	**Lewis *et al.* (1986)** (TKE spectrum)

Medium	x or z	Depth	Location	Value $cm^2 s^{-1}$	Reference/ Comments
Water	Vertical	Pycnocline	Sargasso Sea	0.1 - 1	Jenkins (using heat balance)
Water	Vertical	Pycnocline	Massachusetts Bay	.11 - .14	G. B. Gardner (heat balance)
Water	Vertical	Pycnocline	Massachusetts Bay	0.05	Geyer dye study
Water	Vertical	Pycnocline	S. Cal. Bight	0.05 - 0.6	**Eppley *et al.* (1979)** (using NO_3^- flux)
Water	Kinematic molecular viscosity (diffusion of momentum)			0.01	
Water	Kinematic molecular diffusivity for heat			1.5×10^{-3}	
Water	molecular diffusivity for O_2 & CO_2			$1.5\text{-}2\times10^{-5}$	
Sediment (50% porosity)	molecular diffusivity for O_2 & CO_2			$0.75\text{-}1\times10^{-5}$	
Sediment	Bioturbation rates (particle mixing by animals)			10^{-5} - 10^{-10}	

PROGRAMMING RILEY (1967)

Mills (1989) describes Riley's wonderful gift of writing lucid, crisp prose, which summarized complex mathematical analyses in a few paragraphs. But this gift was also a curse for those who try to figure out how Riley achieved his elegant results. This section, which deals with the mathematical aspects of **Riley's (1967)** model describes how to achieve Riley's results using MATLAB™.

The boxes or states

Riley modeled the New England continental shelf as a set of 6 surface and 6 subsurface boxes, with 25-km horizontal lengths. He doesn't state what the vertical dimensions are for his boxes.

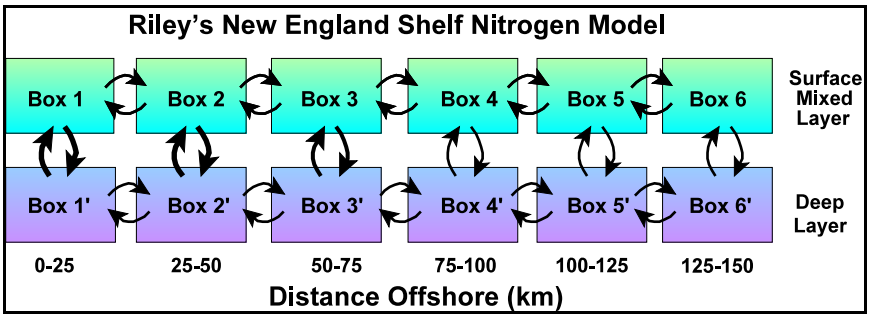

Figure 1. A conceptual view of Riley's 12-box model of the New England shelf.

I'll assume 30 m. Figure 1 provides a conceptual model of Riley's box model.

Riley modeled the transport of Nitrogen and phosphorus between boxes using 1st-order differential equations. The rate of transfer is indicated by the arrows in Fig. 0. These fractional transfer coefficients have dimensions of inverse time, and will be indicated by a_{ij}, where *i* denotes the source and *j* the destination of the transport of N or P. Riley used a simplified form of the advection-diffusion equation to set up the model:

$$\frac{\partial N}{\partial t} = R + \frac{\partial}{\partial x}\left(\frac{A_x}{\rho} \frac{\partial N}{\partial x} \right) + \frac{\partial}{\partial z}\left(\frac{A_z}{\rho} \frac{\partial N}{\partial z} \right).$$

$$\begin{aligned} \textit{where, } A_x &= \textit{dynamic horizontal eddy diffusivity.} \\ A_z &= \textit{dynamic vertical eddy diffusivity.} \\ \frac{\partial}{\partial x} &= \textit{first derivative in x-direction.} \\ \frac{\partial}{\partial z} &= \textit{first derivative in z-direction.} \\ \frac{\partial}{\partial t} &= \textit{local rate of change.} \\ \rho &= \textit{seawater density} \approx 1\ g\,cm^{-3}. \\ R &= \textit{Biological rate of change.} \end{aligned} \qquad \textbf{(3)}$$

Equation 2 states that the local rate of change in a local parcel of water, $\frac{\partial N}{\partial t}$, equals the local production or removal, R, plus the input (or removal) in the horizontal and vertical directions. The final two terms in Equ. 3 are called the eddy diffusion terms. Riley has dropped the advective terms from his equations. Riley's not assuming that currents don't transport N on the continental shelf; they do. He's going to model such transport as a large-scale eddy diffusion problem. These are the assumptions that Riley made in solving this model:

1. the whole system is in steady state
2. the whole system is controlled by nutrient concentration
3. Mixing within boxes is uniform
4. Nutrient transport between boxes controlled by horizontal and eddy diffusivity and biological utilization
5. Horizontal eddy diffusion is uniform throughout the system
6. Vertical eddy diffusion decreases from inshore to offshore

7. N transport due to biological utilization from the surface to deep box = 10% of surface N concentration
8. The ratio of N:P utilization is 15:1
9. Nitrogen & phosphorus concentration in the offshore deep water, Box 6', are constant

Riley estimated the magnitude of horizontal eddy diffusion on the shelf. Riley provides one example of how Equ. 3 can be used to estimate the transport of nitrogen among boxes. He provided the equation for Box 2, the surface 25-50 km box in Fig. 0:

$$\frac{\partial N_2}{\partial t} = R + 0.02\,N_1 + 0.02 N_3 + 0.05 N_2' - 0.09 N_2 . \qquad \textbf{(4)}$$

One of the mysteries in Equ. 4 is the -0.09 N_2 term. Where did it come from? Riley doesn't provide the answer, only that it is obtained by difference: -0.09 = - (0.02 + 0.02 + 0.05). I can provide two explanations to justify such an assumption: one from physical oceanography and one from modeling. If R is zero in the above equation and in the 11 other equations for the N transport if shown in Fig. 0, then at steady-state $\left(\frac{\partial N}{\partial t} = 0.\right)$, the flux into each box must equal the flux out. In physical oceanography, this is known as the continuity assumption. If R=0 in all boxes, then $N_1 = N_1' = N_2 = \ldots = N_{12}$. In the absence of biological utilization, the flux of Nutrient into a box can only equal the flux out if the sum of transfer coefficients is 0. Moreover, in the absence of biological utilization and at steady-state, the nitrogen concentrations in all 12 boxes should be the same, hence the flux in equals the flux out if the sum of the transfer coefficients equal 0.

The second explanation is a little more esoteric. As we shall soon see the transfer coefficients above can be placed in matrix form to solve for the steady-state nitrogen concentrations in each box. If these transfer coefficients sum to zero, then the equations are in closed compartmental form (**Eisenfeld 1979**), which means that in the absence of biological utilization, nitrogen is conserved throughout the model. By having the coefficients sum to 0, Riley ensures that nutrients can neither be created nor destroyed in the absence of biological utilization. I will call this feature of the model, the continuity assumption.

All of the interesting features of Riley's model are generated by biological production. Riley assumed that 10% of the nitrogen from the upper boxes was removed daily by biological production. Riley assumed that this biological loss occurred by sinking of Nitrogen. For Box 2, R = -10% N_2. This removal is in addition to the removal required by the continuity assumption. With this assumption, the equations for Riley's Box 2 (Surface 25-50 km) and subsurface Box 2' are:

$$\begin{aligned}
\frac{\partial N_2}{\partial t} &= 0.02N_1 + 0.02N_3 + 0.05N_2' - 0.09N_2 - 0.10N_2 = 0 \\
&= 0.02N_1 + 0.02N_3 + 0.05N_2' - 0.19N_2 = 0 \\
\frac{\partial N_2'}{\partial t} &= 0.02N_1' + 0.02N_3' + 0.05N_2 + 0.10N_2 - 0.09N_2' = 0 \\
&= 0.02N_1' + 0.02N_3' + 0.15N_2 - 0.09N_2' = 0
\end{aligned} \tag{5}$$

So, Equ. 5 superimposes the biological removal terms on the basic closed compartmental model, producing an additional loss term from the upper box (N_2) and an additional input term to the deep box (N_2'). Each of the coefficients of the sort shown in Equ. 5 are called **fractional transfer coefficients**. These transfer coefficients from box j to box i, called a_{ji}, can be placed in a matrix to solve the 12 steady-state equations for the Riley model:

$$\begin{aligned}
\frac{dN_i}{dt} &= \sum_{j=1}^{c} N_j\, a_{ji} = 0. \\
\dot{N} &= N\,\boldsymbol{A}. \\
\begin{bmatrix} \frac{dN_1}{dt} & \frac{dN_2}{dt} & \cdots & \frac{dN_c}{dt} \end{bmatrix} &= [N_1\ N_2\ \ldots\ N_c]\,\boldsymbol{A}. \\
\begin{bmatrix} 0 & 0 & \cdots & 0 \end{bmatrix} &= [N_1\ N_2\ \ldots\ N_c]\,\boldsymbol{A}.
\end{aligned} \tag{6}$$

Table 2 shows the fractional transfer coefficients, a_{ji}'s.

Table 2. **Riley's (1967)** 100% Nitrogen transfer coefficients, denoted as a_{ij}, where i is the source and j the destination of transport. For consistency with Markov modeling convention, the from rows-to-columns convention is the opposite of that used by Riley. The a_{ij} coefficients have dimensions of d^{-1}. The row sums are 0.

		TO											
		1	**2**	**3**	**4**	**5**	**6**	**1'**	**2'**	**3'**	**4'**	**5'**	**6'**
FROM	**1**	-0.22	0.02	0	0	0	0	0.20	0	0	0	0	0
	2	0.02	-0.19	0.02	0	0	0	0	0.15	0	0	0	0
	3	0	0.02	-0.16	0.02	0	0	0	0	0.12	0	0	0
	4	0	0	0.02	-0.15	0.02	0	0	0	0	0.11	0	0
	5	0	0	0	0.02	-0.15	0.02	0	0	0	0	0.11	0
	6	0	0	0	0	0.02	-0.13	0	0	0	0	0	0.11
	1'	0.10	0	0	0	0	0	-0.12	0.02	0	0	0	0
	2'	0	0.05	0	0	0	0	0.02	-0.09	0.02	0	0	0
	3'	0	0	0.02	0	0	0	0	0.02	-0.06	0.02	0	0
	4'	0	0	0	0.01	0	0	0	0	0.02	-0.05	0.02	0
	5'	0	0	0	0	0.01	0	0	0	0	0.02	-0.05	0.02
	6'	0	0	0	0	0	0.01	0	0	0	0	0.02	-0.03

Modeling K_x and K_z

This matrix of transfer coefficients contains a wealth of information, including the effects of both eddy diffusion and the removal of nitrogen from the surface mixed layer. The horizontal fractional transfer coefficients are 2 % per day (*e.g.*, see $\mathbf{a_{12}}$ and $\mathbf{a_{21}}$ in **Table 2**). **Riley (1967)** states that a 2% daily exchange corresponds to a horizontal kinematic eddy diffusivity of 2.9×10^6 cm^2/sec, but he doesn't explicitly state how he converted from eddy diffusion to fractional transfer coefficients. Riley appears to have used the following relationship to convert K_x and K_z, both with dimensions of $\frac{L}{T^2}$, to an oscillatory flow modeled with fractional transfer coefficients, a_{ij}, with dimensions of $\frac{1}{T}$:

$$
\begin{aligned}
a_{ij} &= \left(\frac{\frac{1}{2} K_x}{(box\ \ length)^2} \right). \\
&= \left(\frac{\frac{1}{2} \frac{2.9 \times 10^6\ cm^2}{s} \times \frac{8.64 \times 10^4\ s}{d}}{(2.5 \times 10^6\ cm)^2} \right). \\
&= 0.02\ d^{-1}.
\end{aligned}
\tag{7}
$$

The conversion shown in Equ. 7 is appropriate and has a long history. The eddy diffusion in the advection-diffusion (=the Fokker-Planck) equation is a phenomenological description of a process that occurs in discrete jumps. The conversion of the diffusion coefficient to probabilities of movement between discrete states was originally due to Einstein and Smoluchuwski.

Riley (1967) did not say what vertical eddy diffusivities were appropriate for his model, nor did he provide the depth of his New England shelf. He modeled the vertical eddy diffusivities to and from the six 25-km wide surface boxes as 10%, 5%, 2%, 1%, 1%, and 1% per day. Assuming a depth of 60 m and Equ. 7, we can calculate the K_z values corresponding to these vertical eddy diffusive transfer coefficients. They are 20.8, 10.4, 5.6, 2.8, 2.8, and 2.8 $cm^2\ s^{-1}$. These K_z values are very high, particularly for the offshore K_z's. Typical oceanic K_z values are from 0.2 to 1 $cm^2\ s^{-1}$ at well-developed pycnoclines (See **Table 1**). In offshore Massachusetts Bay, Bernie Gardner and Rocky Geyer estimated K_z at 0.11 to 0.14 $cm^2\ s^{-1}$. In a later study, Geyer measured the dispersion of dye placed at the pycnocline, which diffused with an apparent K_z of 0.05 $cm^2\ s^{-1}$. This is the lowest K_z value I've found in the literature but it is still two to three thousand times larger than the molecular diffusion coefficient. With a 100-m deep shelf, the K_z values would be decreased by 36%. With a 30-m deep water column, like MA Bay, the K_z values corresponding to Riley's vertical transfer coefficients would be four times greater than that calculated for a 60-m water column.

Modeling new production

Riley didn't explicitly model total production. He assumes that 10% of the dissolved inorganic nitrogen in the surface mixed layer is advected to depth each day due to biological processes. At steady-state, which by definition means a constant N concentration in each box, the new production in units of nitrogen could be estimated by: New production = $a_{i\,i,} \times N_i$. This rate of New Production in units of Nitrogen, could be converted to units of Carbon by using a Redfield ratio for C:N, or ≈6.6.

The downward diffusive transport of N by biological production is added to the downward transport of N due to eddy diffusion. In Box 1, this downward transport is 20% per day (10% for vertical eddy diffusive transport, and 10% for new biological production), but the upward vertical transport is only 10% of the concentration in the deep box per day (vertical eddy diffusive

transport only). Equation 5 shows that for Box 2, the downward transport is 15% per day compared to an upward transport of only 10% per day.

The closed compartmental (ergodic Markov) Nitrogen model

Riley's model is completely described by the elements of the **A** matrix, shown in **Table 2**. Recall that the negative elements along the main diagonal are required by the continuity assumption. **Eisenfeld (1979)** provides a good description of the properties of compartmental models such as Riley's. A closed system in which no nitrogen is lost must have the row sums of the transfer matrix equal zero. All of the transfer coefficients in the off diagonal elements must be non-negative. Like Charlie on the MTA, a mole of nitrogen in this model cycles forever.

Riley (1967) set one boundary condition for his model: the concentrations of N and P in the deep, offshore Box 6' would remain constant at 15 and 1 μM. With this condition, the steady-state concentration of nitrogen can be solved using Runge-Kutta integration of the twelve coupled first-order differential equations described by **Equ. 6**. MATLAB™ performs a numerical integration of these coupled differential equations using the Runge-Kutta algorithm (ode45).

Eisenfeld (1979) showed how closed compartmental models, such as Riley's, could be converted to a Markov chain model. Recall that the a_{ij} values of dimensions of inverse time. A Markov chain transition matrix provides the probability that a system in state i will be in state j in the next time step. One can regard the transition matrix as expressing the probability that 1 atom of N will move from one box to another in a given time period. If **A** is the matrix of fractional transfer coefficients, the Markov chain transition probability matrix can be calculated using the matrix exponential function, shown in Equation 6:

$$\begin{aligned} \mathbf{P}(h) &= e^{h\mathbf{A}} = \mathbf{I} + h\mathbf{A} + \frac{h^2\mathbf{A}^2}{2!} + \ldots \\ \textit{where, } \mathbf{A} &= \textit{fractional transfer coefficient matrix.} \\ h &= \frac{\textit{Markovian } \mathbf{P} \textit{ timestep}}{\mathbf{A} \textit{ timestep}}. \\ \mathbf{I} &= \textit{Identity matrix.} \\ \mathbf{P} &= \textit{Markov transition probability matrix.} \end{aligned} \qquad \textbf{(6)}$$

If the fractional transfer coefficients are expressed as d^{-1}, then a 1-day transition matrix could be calculated by setting *h* in Equ. 6 to 1. For a weekly transition Probability matrix, *h* should be 7. For an hourly transition matrix, *h* should be $\frac{1}{24}$. For short time periods, $P \approx I + h\,\mathbf{A}$, but this approximation does not take into account that the system could move between multiple states in a single time step. Moler (199x) describes the many dubious ways to calculate the matrix exponential. MATLAB™, founded by Cleve Moler, has a built in function, expm.m, which solves for the matrix exponential:

```
P=expm(A);   % The matrix exponential converts to Markov
             % transition matrix (Eisenfeld 1979);
```

Table 3 shows the Markov transition matrix for the fractional transfer coefficient matrix, **A**, shown in **Table 2**. As in all Markov transition probability matrices, the row sums equal unity. Some of the differences between Tables 2 and 3 point out some key differences between fractional transfer coefficient matrices and transition probability matrices. For example, in Table 2 the fractional transport between Box 1 and Box 1' is 20% daily, and yet the transition probability in Table 3 is only 16.9%. The 20% in Table 2 is a parameter for a continuous time process in which the 20% is the coefficient for a 1st order differential equation:

$$\frac{dN_1'}{dt} = 20\% \; N_1 + \ldots . \qquad (7)$$

The 16.9% in **Table 3** is the solution for this equation at the end of exactly 1 day. During this day, the instantaneous rate of transfer of N is 20% daily, but at the end of the day some of this nitrogen has returned from Box 1' to Box 1, some has moved to Box 2', and some has even moved from Box 2' to Box 2. The transition probabilities in **Table 3** represent the integration of 12 coupled first-order ordinary differential equations. I can perform this integration after a week by simply changing the timestep, *h*, in Equ. 6 from one to seven. The weekly transition matrix is shown in **Table 4**. More off-diagonal transition probabilities are greater than 0.001 as one could expect from integrating the instantaneous 1-step transitions described completely by the transfer coefficients in **Table 2**.

Table 3. The 1-day regular ergodic Markov transition probability matrix corresponding to the fractional transfer coefficient matrix shown in **Table 2**. The transition probabilities are dimensionless. Probabilities less than 0.001 are rounded to 0. The stable limit or fixed point probability vector (**Kemeny & Snell 1976**, p. 70; **Roberts 1976**, p 291), **α**, is also shown.

FROM \ TO	1	2	3	4	5	6	1'	2'	3'	4'	5'	6'
1	0.811	0.016	0	0	0	0	0.169	0.003	0	0	0	0
2	0.016	0.831	0.017	0	0	0	0.003	0.131	0.002	0	0	0
3	0	0.017	0.854	0.017	0	0	0	0.002	0.108	0.002	0	0
4	0	0	0.017	0.862	0.017	0	0	0	0.002	0.100	0.002	0
5	0	0	0	0.017	0.862	0.017	0	0	0	0.002	0.100	0.002
6	0	0	0	0	0.017	0.879	0	0	0	0	0.002	0.102
1'	0.085	0.001	0	0	0	0	0.896	0.018	0	0	0	0
2'	0.001	0.044	0.001	0	0	0	0.018	0.918	0.019	0	0	0
3'	0	0.001	0.018	0	0	0	0	0.019	0.943	0.019	0	0
4'	0	0	0	0.009	0	0	0	0	0.019	0.952	0.019	0
5'	0	0	0	0	0.009	0	0	0	0	0.019	0.952	0.019
6'	0	0	0	0	0	0.009	0	0	0	0	0.019	0.971
α	0.055	0.041	0.025	0.015	0.014	0.014	0.112	0.125	0.142	0.151	0.153	0.153

Table 4. The 7-day regular ergodic Markov transition probability matrix corresponding to the fractional transfer coefficient matrix shown in **Table 2.**

FROM \ TO	1	2	3	4	5	6	1'	2'	3'	4'	5'	6'
1	0.364	0.047	0.003	0	0	0	0.513	0.067	0.005	0	0	0
2	0.049	0.335	0.047	0.003	0	0	0.065	0.436	0.060	0.004	0	0
3	0.003	0.049	0.358	0.050	0.004	0	0.004	0.058	0.413	0.057	0.004	0
4	0	0.003	0.051	0.369	0.051	0.004	0	0.004	0.056	0.402	0.056	0.004
5	0	0	0.004	0.051	0.369	0.055	0	0	0.004	0.056	0.402	0.060
6	0	0	0	0.004	0.055	0.420	0	0	0	0.004	0.060	0.457
1'	0.256	0.027	0.001	0	0	0	0.621	0.087	0.006	0	0	0
2'	0.029	0.145	0.014	0.001	0	0	0.085	0.626	0.092	0.007	0	0
3'	0.002	0.016	0.069	0.007	0	0	0.006	0.091	0.702	0.100	0.007	0
4'	0	0.001	0.008	0.037	0.005	0	0	0.007	0.099	0.734	0.102	0.007
5'	0	0	0	0.005	0.037	0.005	0	0	0.007	0.102	0.735	0.109
6'	0	0	0	0	0.005	0.042	0	0	0	0.007	0.109	0.836

Regular ergodic Markov processes have the property that no matter what the initial state, the system eventually converges on a stable solution, called the stable limit or fixed point probability vector, designated **α**. This ergodic property produces the following equality (*n.b.*, α is a row vector):

$$\boldsymbol{\alpha} = \boldsymbol{\alpha}\,\mathbf{P}. \qquad \textbf{(8)}$$

To find this steady-state solution, there are at least three different options:

- Raise the P matrix to higher & higher powers, producing a matrix with all rows equal to **α**.
- Solve for the eigenvector associated with the dominant eigenvalue of 1, and scale this eigenvector so that the sum equals unity.
- Use the following MATLAB™ program to solve a set of c simultaneous linear equations, for a c × c transition matrix. I wrote this algorithm to solve the characteristic equation of a matrix to solve for the eigenvector associated with an eigenvalue of 1.0, but the same set of linear equations result from solving Equ. 8 directly.

```
% P defines a regular, ergodic Markov chain
% The stable limit vector, α, is the eigenvector associated with
% the dominant eigenvalue in a regular ergodic chain (=1 by def), This
% eigenvector must be scaled such that the sum of elements=1.
% Solve for the eigenvector and scale simultaneously using the
```

```
% characteristic equation:
%     The characteristic equation for a matrix:
%     (λ*I-P') * α      =     0
%                 PT*α  =     B
%     where,      λ     =     eigenvalue
%     If λ=1, α   =     the Markovian stable limit vector.
PT=I-P';    % The key term of characteristic equation (λ=1)
% Replace final row of PT with a row of ones to scale to 1
PT(states,:)=ones(1,states);
B=[zeros(states-1,1);1];
% solve for n unknowns with n simultaneous linear equations
α=(PT\B)';
%     X     =     A\B is MATLAB solution to AX=B
%                 then convert α to row vector
```

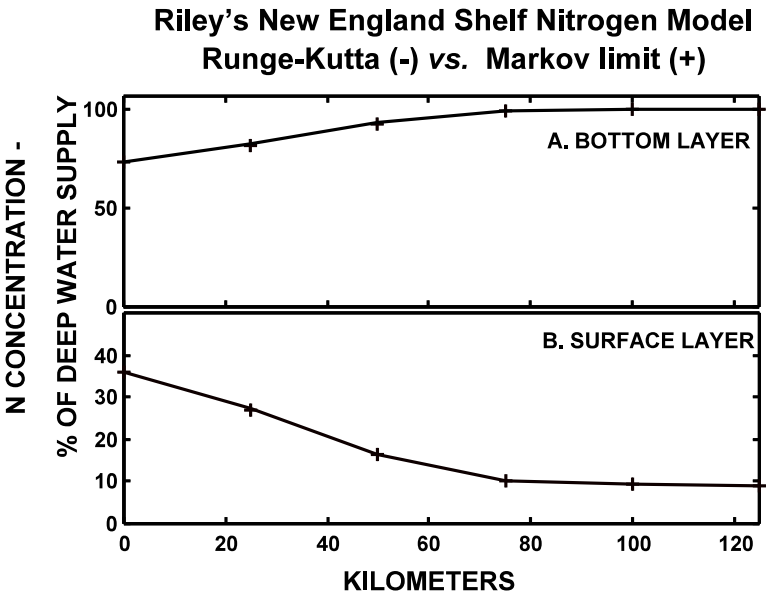

Figure 1 The steady-state solution of Riley's model with 100% N regeneration in bottom waters. Runge-Kutta integration and regular ergodic Markov chain theory produce identical steady-state solutions. The model has a boundary condition that the offshore deep box (Box 6') has a constant 15 µM N concentration.

The final choice, solving a set of simultaneous linear equations, is the fastest and produces an **α**, showing the fraction of total N in each box. The **α** vector is shown in **Table 3**. This vector can be scaled so that Box 6' is 15 µM N to produce the steady-state solution, which is identical to that produced by numerical integration of the 12 coupled first-order ordinary differential equations (Fig. 1)

Figure 1B shows a key, non-intuitive feature of **Riley's (1967)** model. Surface nitrogen concentration drops more than three-fold from in- to off-shore, seemingly indicating an inshore source of Nitrogen. But recall, the only source of Nitrogen in this model is the offshore deep box. In this model, Riley did not distinguish among the different forms of Nitrogen, so the in-to-offshore gradient could include both dissolved inorganic, dissolved organic, and particulate organic nitrogen.

Table 5 shows the mean first passage times for nitrogen in this regular ergodic Markov process. These first-passage times are not residence times. They are can be interpreted as follows: "Once a molecule of nitrogen leaves a compartment, how long, on average, will it take that molecule to reach another compartment including returning to the original compartment?" The mean first passage times in **Table 5** are long. It takes, on average, a single nitrogen molecule about one week to return to the deep offshore boxes (2' to 6') once they have been dispersed from their original boxes. It takes 18 days for an N molecule to return to the inshore surface box (1') once it has left that box. It takes an extraordinary 1264 d for a N molecule to leave the inshore boxes and arrive at the offshore surface box. The variances on these probabilities are extraordinarily high, so it is possible for an N molecule to make this trip relatively rapidly, but it is also highly likely

that a single N molecule might take an extraordinarily long time to make the transit from inshore to offshore. It is important to note that these are **mean** first passage times. How can it take 33 days for the average nitrogen molecule to travel from box 1 to 1' when 20% of the nitrogen molecules are transferred daily between Box 1 and Box 1' (**Table 2**)? The answer lies in the fact that some molecules are transferred horizontally to Box 2 and these may make a very long random walks in both the surface and deep boxes before arriving at Box 1'.

Table 5. The mean first passage time matrix for N (100% Nitrogen regeneration) [days] (**Kemeny & Snell 1976**, p. 78; **Roberts 1976**, p. 295)

		TO											
		1	**2**	**3**	**4**	**5**	**6**	**1'**	**2'**	**3'**	**4'**	**5'**	**6'**
FROM	**1**	18	126	339	684	949	1264	33	67	164	311	508	757
	2	299	24	277	632	899	1214	263	38	116	261	458	707
	3	503	291	40	500	794	1113	461	212	44	164	358	607
	4	654	450	354	65	601	957	611	359	162	46	212	458
	5	754	551	477	471	71	705	711	459	257	112	46	263
	6	804	601	530	563	448	72	761	508	307	158	62	51
	1'	67	133	340	684	949	1264	9	65	164	310	508	757
	2'	304	115	296	636	899	1214	261	8	113	260	458	707
	3'	504	302	250	547	801	1114	461	208	7	159	357	607
	4'	654	452	383	455	659	966	611	358	156	7	207	457
	5'	754	551	481	525	496	771	711	458	257	106	7	257
	6'	804	601	531	571	513	560	761	508	307	157	56	7

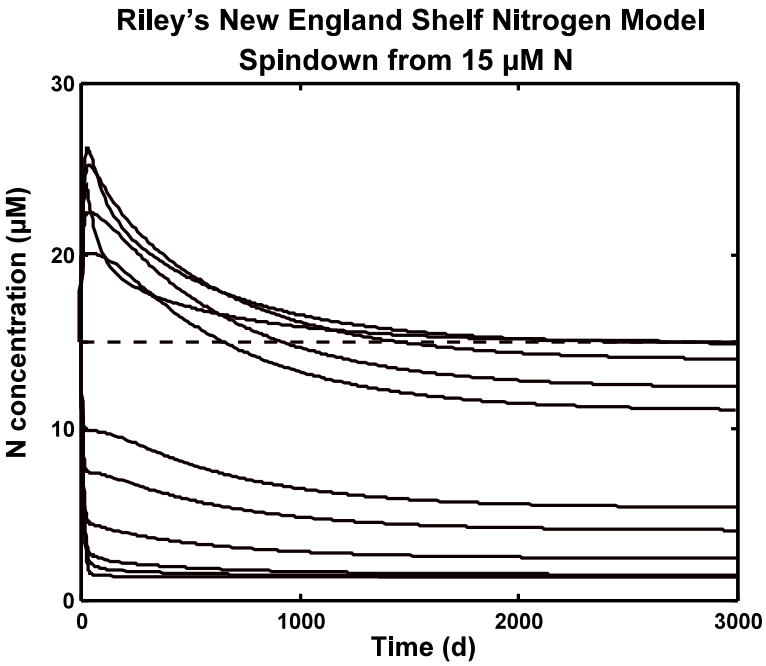

Figure 2. Starting at 15 µM N, typical late-winter concentrations for the shelf, the model takes an unrealistic 3000 d to attain steady-state.

It takes a long time for the numerical integration to converge if the initial concentrations differ substantially from the steady-state solutions. Starting at 15 µM N in each box, the system takes roughly 3000 days to reach steady-state (Fig. 2).

The open compartmental (absorbing Markov) denitrification model

Riley (1967) designed this model to provide a parsimonious explanation for nitrogen rather than phosphorus being the limiting nutrient in coastal waters. He also wanted to explain why the N:P ratio attained such low values in coastal waters. To do that, Riley added one simple component to the model: the loss of Nitrogen in bottom waters. Although denitrification was never mentioned by Riley, we now know, as **Brandt (1899)** suspected, that denitrification in bottom waters leads to Nitrogen limitation of coastal and all oceanic waters.

To model incomplete Nitrogen regeneration in bottom waters, Riley ran his model with 50%, 60%, 70%, 80%, and 100% N regeneration. In this model, N is removed from the surface box, but not all of this N appears in the bottom waters to be ultimately returned to the surface. In order to model this process, I made box 6' an excretory box in **Eisenfeld's (1979)** terminology. **Table 6** shows the fractional transfer coefficient matrix for 80% N regeneration. **Table 7** shows the 1-day transition matrix corresponding to these fractional transfer coefficients.

Table 6. **Riley's (1967)** 80% Nitrogen transfer matrix. The fractional transfer coefficients that differ between this matrix and that in **Table 2** are bolded. In this version of the model, I have modeled box 6' as an excretory state (an absorbing state in Markov terminology), a state which receives the N lost from the incomplete N regeneration. Before conversion to an absorbing Markov model, the transfer coefficients **from** Box 6' are changed to 0s.

		TO											
		1	**2**	**3**	**4**	**5**	**6**	**1'**	**2'**	**3'**	**4'**	**5'**	**6'**
FROM	**1**	-0.22	0.02	0	0	0	0	**0.18**	0	0	0	0	**0.02**
	2	0.02	-0.19	0.02	0	0	0	0	**0.13**	0	0	0	**0.02**
	3	0	0.02	-0.16	0.02	0	0	0	0	**0.10**	0	0	**0.02**
	4	0	0	0.02	-0.15	0.02	0	0	0	0	**0.09**	0	**0.02**
	5	0	0	0	0.02	-0.15	0.02	0	0	0	0	**0.09**	**0.02**
	6	0	0	0	0	0.02	-0.13	0	0	0	0	0	**0.11**
	1'	0.10	0	0	0	0	0	-0.12	0.02	0	0	0	0
	2'	0	0.05	0	0	0	0	0.02	-0.09	0.02	0	0	0
	3'	0	0	0.02	0	0	0	0	0.02	-0.06	0.02	0	0
	4'	0	0	0	0.01	0	0	0	0	0.02	-0.05	0.02	0
	5'	0	0	0	0	0.01	0	0	0	0	0.02	-0.05	0.02
	6'	0	0	0	0	0	0.01	0	0	0	0	0.02	-0.03

This excretory compartmental model can be translated into an absorbing Markov model, with state 6' as the absorbing state. However, the deep offshore box isn't really an absorbing state. Nitrogen from that box fuels the entire model. It was just mathematically more convenient to handle Box 6' as an absorbing state. We'll deal with the input of deep N in a moment.

Table 7. The absorbing Markov transition probability matrix corresponding to the fractional transfer coefficient matrix (80% N regeneration) shown in **Table 6**. The matrix has been placed in canonical form (Equ. 9). Box 6' is an absorbing state, a state once entered that can never be left. Fluxes out of this state to adjoining states will be handled using a pulse input vector, ***f***. The pulse input vector ***f*** is shown at the bottom of the Table. Also shown is the steady-state N concentration vector, generated by Equ. 11 (see text). Transition probabilities less than 0.001 are rounded to 0.

		TO											
		6'	**1**	**2**	**3**	**4**	**5**	**6**	**1'**	**2'**	**3'**	**4'**	**5'**
FROM	**6'**	1.0	0	0	0	0	0	0	0	0	0	0	0
	1	0.018	0.810	0.016	0	0	0	0	0.152	0.003	0	0	0
	2	0.019	0.016	0.830	0.017	0	0	0	0.003	0.113	0.002	0	0
	3	0.019	0	0.017	0.853	0.017	0	0	0	0.002	0.090	0.002	0
	4	0.019	0	0	0.017	0.861	0.017	0	0	0	0.002	0.082	0.002
	5	0.021	0	0	0	0.017	0.861	0.017	0	0	0	0.002	0.082
	6	0.103	0	0	0	0	0.017	0.878	0	0	0	0	0.001
	1'	0.001	0.085	0.001	0	0	0	0	0.895	0.018	0	0	0
	2'	0	0.001	0.044	0.001	0	0	0	0.018	0.917	0.019	0	0
	3'	0	0	0.001	0.018	0	0	0	0	0.019	0.943	0.019	0
	4'	0	0	0	0	0.009	0	0	0	0	0.019	0.952	0.019
	5'	0.020	0	0	0	0	0.009	0	0	0	0	0.019	0.952
	f		0	0	0	0	.0027	.1386	0	0	0	.0029	.2884
	c	15.00	0.94	0.93	0.81	0.74	0.98	1.29	1.87	2.82	4.80	7.53	10.69

All absorbing Markov transition probability matrices can be rewritten in canonical form, by listing the absorbing states first:

$$\mathbf{P} = \left[\begin{array}{c|c} \boldsymbol{I} & \mathbf{0} \\ \hline \boldsymbol{Q} & \boldsymbol{R} \end{array} \right]. \qquad \textbf{(9)}$$

The transition probability matrix can be partitioned into four submatrices:

- **I** the identity matrix corresponding to the absorbing states
- **O** a matrix of all zeros
- **Q** the transitions among the transient or non-absorbing states
- **R** the transitions from non-absorbing or transient states to the absorbing states

The fundamental matrix, **N**, of absorbing Markov chain theory is:

$$\mathbf{N} = (\mathbf{I} - \mathbf{Q})^{-1}. \quad (10)$$

Roberts (1976) following **Kemeny & Snell (1976)** showed that the steady-state concentration vector, **c**, for an absorbing Markov process receiving a pulsed input **f** of a substance into one or more transient states at every timestep is:

$$\mathbf{c} = \mathbf{f}\,\mathbf{N}. \quad (11)$$

Riley (1967) probably didn't solve for the steady-state solution of his model using this approach, but he did provide the appropriate information to model the process this way. The only source of Nitrogen in the model, to replenish that lost by denitrification is from Box 6', the offshore deep box. This pulse input vector is simply the final row of the regular ergodic N transition probability matrix (**Table 3**) times the deep-water N supply, or P_{12}.× 15 µM. While Box 6' only has direct connections to Box 6 and Box 5', due to the higher powers of the matrix exponential (Equ. 6), some pulse input goes into boxes 5 and 4' as well.

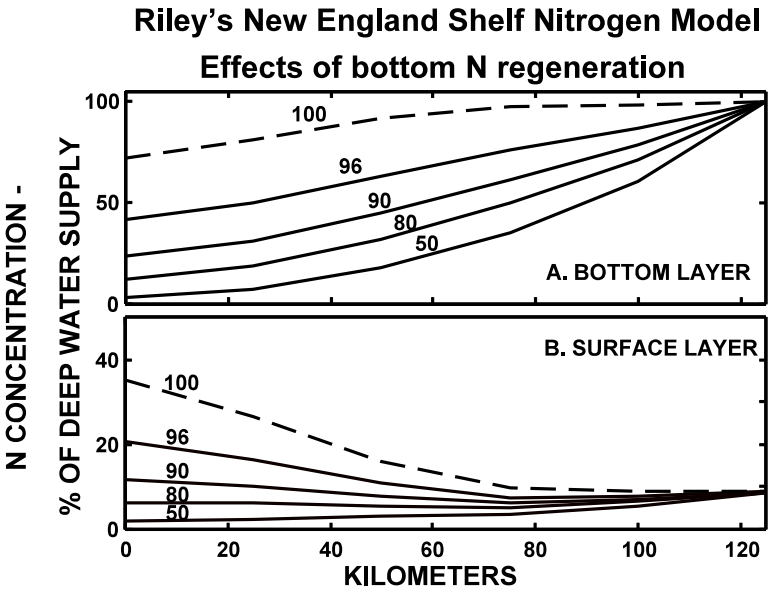

Figure 3 An absorbing Markov model solution of **Riley's (1967)** model. This figure matches Riley's Fig. 1, except for the 100% N regeneration curve (see text). For his coupled N and P model, Riley assumed that there was 80% N regeneration.

Figure 3 shows the steady-state concentrations of Nitrogen with different rates of Nitrogen regeneration. This figure matches Riley's Fig. 1 quite closely, with one noted exception: Riley's 100% N regeneration curve is better represented by a 96% N regeneration curve. I suspect that the difference is due to the Markov model's more accurate calculation of steady state. Riley chose to use the 80% N regeneration in his later analysis of N:P ratios.

The model shows a few interesting features of continental shelf N distribution. At 80% regeneration, nitrogen is drastically depleted throughout the surface layer. The key process driving shelf production in this model is the offshore-to-inshore bottom nitrogen gradient, shown in Fig. 3A.

N:P ratios: Coupling an absorbing N and ergodic P model

Riley (1967) modeled the cross-shelf gradient in phosphorus and N:P ratios, but he provided no details on how he accomplished this task and generated his Figure 2. The key to the modeling nitrogen limitation on the shelf is that Nitrogen was assumed to have only 80% N regeneration while phosphorus had 100% N regeneration. Thus, the steady-state P concentration could be modeled with a 12 × 12 regular ergodic transition probability matrix, with the physical mixing terms identical to those used for nitrogen (see **Table 3**). There is a nasty twist however. The biological removal coefficients from the upper to lower boxes for N and P must be in Redfield proportions. Riley assumed the N:P ratio in phytoplankton production was 15. Now recall that Riley assumed that 10% of the daily concentration of N was removed each day. I can't simply divide this 10% of 15 to produce the biological removal of P. The biological removal of N, 10% × C_N, where C_N is the steady-state concentration must equal the biological removal probability for phosphorus times the steady-state concentration of phosphorus. The tricky part is that we don't know either the transition probability or the steady-state P concentration. However we are aided by the fact that of the 144 transition probabilities in the 12 × 12 Phosphorus transition probability matrix, there are only 6 unknowns. These are the transitions from Box 1 to Box 1', Box 2 to 2', Box 3 to 3', Box 4 to 4', Box 5 to 5', and Box 6 to 6'. The values for these transition probabilities determine the standing stock of P in each of the 12 boxes. Since we already know the removal rate of Nitrogen, we simply have to use an iterative procedure to find the combination of these 6 transition probabilities that produce a P flux that is one fifteenth as large as the N flux. I used MATLAB™'s fmins routine to find the Phosphorus transition probabilities that would produce a 15:1 N:P flux in these 6 boxes. It takes about 5 minutes of Pentium computer time to produce a solution with 1×10^{-13} precision. That transition matrix is shown in **Table 8**.

Table 8. The regular ergodic Markov transition probability matrix for phosphorus. The stable limit vector **α** is the fraction of the total phosphorus in each box. The steady-state concentration is **c**, which is **α** scaled so that Box 6' is 1 μM . The six bolded transition probabilities were determined by an iterative search (using Matlab's fmins function) for the combination that produced a 15:1 N:P downward flux in boxes 1 to 5 (see text).

		TO											
		1	**2**	**3**	**4**	**5**	**6**	**1'**	**2'**	**3'**	**4'**	**5'**	**6'**
FROM	**1**	**0.883**	0.018	0	0	0	0	**0.098**	0.002	0	0	0	0
	2	0.018	**0.906**	0.018	0	0	0	0.002	**0.055**	0.001	0	0	0
	3	0	0.018	**0.932**	0.019	0	0	0	0.001	**0.029**	0.001	0	0
	4	0	0	0.019	**0.940**	0.019	0	0	0	0.001	**0.021**	0	0
	5	0	0	0	0.019	**0.932**	0.019	0	0	0	0	**0.029**	0.001
	6	0	0	0	0	0.019	**0.939**	0	0	0	0	0.001	**0.041**
	1'	0.088	0.001	0	0	0	0	0.892	0.018	0	0	0	0
	2'	0.001	0.045	0.001	0	0	0	0.018	0.916	0.019	0	0	0
	3'	0	0.001	0.019	0	0	0	0	0.019	0.942	0.019	0	0
	4'	0	0	0	0.009	0	0	0	0	0.019	0.952	0.019	0
	5'	0	0	0	0	0.009	0	0	0	0	0.019	0.952	0.019
	6'	0	0	0	0	0	0.010	0	0	0	0	0.019	0.971
	α	0.079	0.074	0.064	0.053	0.042	0.034	0.088	0.093	0.102	0.114	0.124	0.132
	c	0.596	0.561	0.487	0.397	0.320	0.260	0.665	0.700	0.773	0.864	0.941	1.000

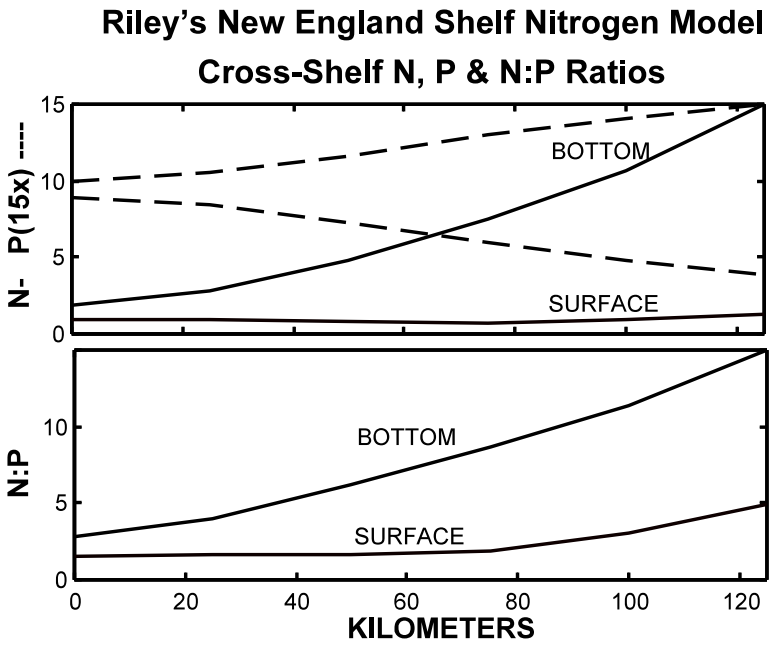

Figure 4 The results of the coupled absorbing (N) and regular ergodic (P) Markov chain models. The results match **Riley's (1967)** Fig. 2 closely.

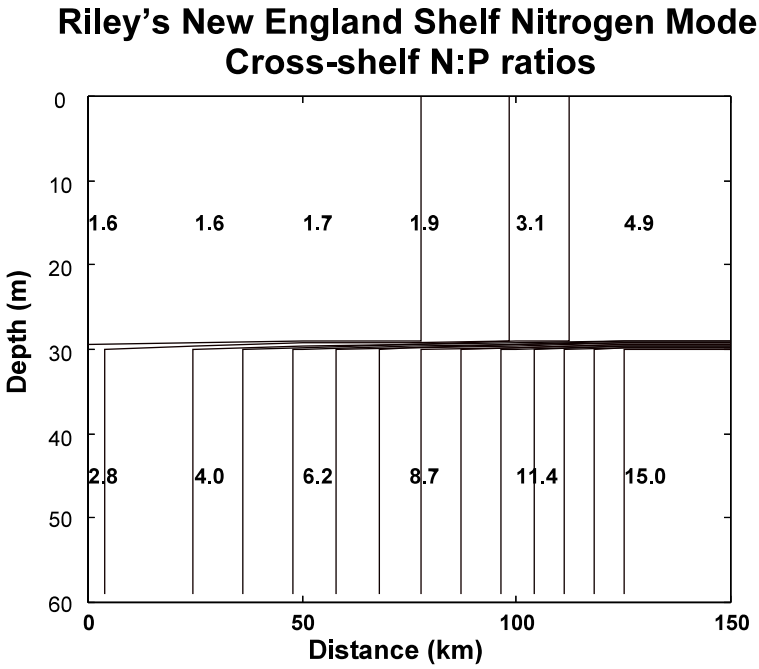

Figure 5 The cross-shelf gradient in N:P ratios are shown. Interestingly, the lowest N:P ratios are in the nearshore surface zone. If N:P ratios decline much below 15, Nitrogen will be the nutrient limiting phytoplankton growth.

Figure 4 shows the results of the coupled N and P model. It shows the nearly complete depletion of nitrogen in surface waters. Figure 4B shows the striking decrease in N:P ratios as one moves from offshore deep to nearshore deep waters. The C:N ratio is further depleted in the surface mixed zone.

Figure 5 shows a different way of plotting the same data. This figure emphasizes that the major mode of transport is cross-shelf along the bottom, up at the coast and out at the surface.

Implications of Riley's Model for MA Bay

Adams *et al.*(1992) solved one of the major unanswered questions about nutrient loading to MA Bay, using principles very similar to those in **Riley's (1967)** model. John Christianson, at Maine's Bigelow Institute, had argued that the MWRA outfall would lead to a major increase in the nitrogen loading to MA Bay. Christianson argued that much of the nitrogen entering Boston Harbor was being lost via denitrification. When the outfalls were moved offshore, denitrification rates would probably not be as high, leading to a much higher nitrogen loading to the euphotic zone. **Adams *et al.*(1992)** used a closed compartmental model to show that the vast majority of nitrogen loading to MA Bay is from offshore, deep water and not from the Boston Harbor outfalls. Even if the rates of denitrification in the harbor were high, little increase in nitrogen loading would result from the location of the new outfalls.

Since Adams's paper, Anne Giblin and Brian Howes have obtained many

estimates of denitrification rates in Boston Harbor and Massachusetts Bay sediments. Up to 75% of the particulate organic nitrogen that enters some Boston Harbor sediments is eventually lost as N_2 gas via denitrification. Modeling by Rich Signell (and others) has shown the basic ideas found in Riley's general model to be true. The major source of nitrogen input to the coastal zone is from offshore deep water. This deep water tends to have N & P in Redfield proportions, but as it traverses the shelf, denitrification leads to increasing nitrogen depletion.

Eppley *et al.* (1979)'s test of N coupling in S. California

LOGICAL FALLACIES

The study by **Eppley *et al.*(1979)** is rightfully praised for a number of reasons including its application of a variety of new methods for assessing nitrogen uptake by phytoplankton and its coupling of physical and biological processes using the advection-diffusion equation. On p. 484, Eppley *et al.* (1979) propose a null hypothesis that primary production is independent of nitrogen supply, and they apply four tests. The rejection of null hypothesis is the heart of the scientific method. Popper (1959) was the philosopher of science who based his entire scientific method on the principle of falsificationism and the *modus tollens*. The *modus tollens* is the logical syllogism that states, "If A then B, not B, conclude not A." In this logical syllogism, A is the null hypothesis, and science advances by rejecting it (usually with statistical tests). If the field data seems to support the null hypothesis, then one can conclude nothing about the truth of A. The logical fallacy known as "affirming the consequent" is "If A then B, B, conclude A." If primary production is controlled by iron, then all phytoplankton cells must require iron. If one finds that all phytoplankton cells require iron, one cannot conclude that iron controls phytoplankton growth. The following chart indicates the role of statistical tests and null hypotheses:

		Null Hypothesis True	**Null Hypothesis False**
DECISION BASED ON STATISTICAL TEST	**Reject H_o**	**Type I error**	**Correct Decision** "Science Advances"
	Accept H_o	**Correct Decision** "No Advance"	**Type II Error**

Eppley *et al.* (1979, p. 484) describe their main hypothesis and their null hypothesis

> *"The hypothesis that the transport of nitrate into the euphotic zone regulates the production of phytoplankton in southern California coastal waters is not easily proved. However, the null hypothesis that the input of nitrate is independent of phytoplankton production*

> *may be tested in several ways, some of which have already been implied."*

Now, there are some tricky logical fallacies involved in accepting an experimental design based on these two sentences. Eppley *et al.* (1979) are correct that hypotheses cannot be proven in the empirical sciences; proofs are the foundation of mathematics, but all but impossible in the empirical sciences. Eppley *et al.*(1979) propose a reasonable null hypothesis for testing, "*the input of nitrate is independent of phytoplankton production* (in southern California coastal waters)*."* However, rejection of this null hypothesis does not allow Eppley *et al.*(1979) to accept their alternate hypothesis, *"the transport of nitrate regulates the production of phytoplankton in southern California coastal waters."* The reason why rejection of the null doesn't entail this alternate hypothesis is that there are many alternate hypotheses to their null hypothesis. These include:

- Primary production is controlled by light and mixing depth. Increasing light or reduced mixing depths result in higher nitrate uptake creating a steeper nitrogen concentration gradient that increases the vertical and horizontal fluxes of nitrate
- Primary production rate is controlled (in the Liebigian sense) by phosphorus, iron, zinc, or silica. Increased growth controlled by one of these limiting nutrients is associated with increased nitrate uptake as well.

There are many other alternate hypotheses that can be devised. See if you can create some alternate hypotheses that are consistent with a rejection of the null hypothesis and that are consistent with the data.

Eppley *et al.* (1979, p 485) restate their null hypothesis and introduce 3 'subordinate null hypotheses':

> *" ... the null hypothesis — phytoplankton production is independent of the rate of nitrate input to the euphotic zone — will be examined in terms of three subordinate null hypotheses. 1) There is no relation between the carbon and nitrate assimilation rates of the plankton and the system runs on other N sources, such as ammonia from regeneration. 2) Temporal and spatial differences in nitrate input rate are independent of phytoplankton production rates. 3) Calculations of diffusive nitrate transport based on nitrate concentration gradients and nitrate assimilation rates will give unrealistic results."*

Now, there are some real logical problems in the introduction of these 'subordinate' null hypotheses. The logical syllogism that the authors want you to follow is, "We reject the 'subordinate null hypothesis', therefore we can reject the (main) null hypothesis "*— phytoplankton production is independent of the rate of nitrate input to the euphotic zone —"* and we can accept the alternative hypothesis *"the transport of nitrate into the euphotic zone regulates the production of phytoplankton in southern California coastal waters."* In the previous paragraph, examples are provided to show that one cannot accept the alternate hypothesis even if the main null hypothesis is rejected.

The first subordinate hypothesis that *1) There is no relation between the carbon and nitrate assimilation rates of the plankton and the system runs on other N sources, such as ammonia from regeneration*. This subordinate hypothesis is a straw man. Let's imagine a situation where the major phytoplankton groups grow mainly on urea and ammonia, but can take up some nitrate. There will be an association between nitrate uptake and carbon assimilation, allowing the investigators to reject subordinate hypothesis 1. This doesn't allow the investigators to either reject the main null hypothesis nor to proceed one step further and accept the alternate hypothesis of nitrate flux controlling production. The rate of nitrate input to the euphotic zone may be so large that it is not substantially affected by the uptake of nitrate by phytoplankton, even though in incubation bottles there is a statistical association between nitrate uptake and carbon fixation.

The second subordinate hypothesis is "*2) Temporal and spatial differences in nitrate input rate are independent of phytoplankton production rates*." This subordinate hypothesis is very close to the main null hypothesis "*— phytoplankton production is independent of the rate of nitrate input to the euphotic zone —"*. Rejection of the subordinate is logically consistent with rejection of the main null hypothesis. However, rejection of this subordinate hypothesis doesn't allow the investigators to accept the alternate hypothesis that nitrate input regulates primary production. Another alternate hypothesis is that production is controlled by light or another nutrient and that production controls the diffusive flux of nitrate. More production implies more nitrate uptake which increases the nitrogen concentration gradient which would increase the diffusive flux.

The third subordinate hypothesis is *"3) Calculations of diffusive nitrate transport based on nitrate concentration gradients and nitrate assimilation rates will give unrealistic results*" This hypothesis has the most complex structure of the three. As we will see, this hypothesis is based on applying the advection-diffusion equation. The others use the nitrate concentration gradient and the assimilation rate of nitrate to estimate the vertical kinematic eddy diffusivity, K_z. If their estimate of K_z was close to literature values for K_z (see my **Table 1**), then they reject the subordinate null hypothesis 3, and the main null hypothesis. Imagine a situation where the model estimates are grossly in error ($K_z < 0.01$ cm^2s^{-1} or $K_z > 5$ cm^2s^{-1}). The authors would be forced to accept their null hypothesis. They should not accept their main null hypothesis, nor can they reject their alternate hypothesis. This would be committing the fallacy of "assuming the consequent." The unrealistic result might be due to an inappropriate use of the advection-diffusion equation. For example, Eppley *et al.*(1979) assume that the major flux of nitrate to the euphotic zone is vertical. A strong case could be made that the major flux of nitrate is horizontal. Indeed, that is one of the major conclusions of Riley's (1967) box model of the continental shelf. Their K_z estimates could be greatly in error, and yet their main null hypothesis "*— phytoplankton production is independent of the rate of nitrate input to the euphotic zone"* could be false (production is controlled by nitrate input, but the major flux could be horizontal). Eppley *et al.*(1979) calculate K_z values that are reasonable, and they reject their null hypothesis of 'unrealistic values' and reject the main null hypothesis. However, it is very possible that a erroneous or inadequate model occasionally gives accurate results. Fortunes have been lost on Wall Street by investors forgetting this principle. Inferring that an accurate prediction implies that the model is 'correct' is yet another example of "assuming the consequent." We can imagine that primary production is driven largely by horizontal advection of ammonia or urea. An inappropriate use of the advection diffusion equation could produce a K_z value falling between

0.05 and 5 cm^2s^{-1}, leading to rejection of the subordinate null, rejection of the main null, and acceptance of the alternate hypothesis *"the transport of nitrate into the euphotic zone regulates the production of phytoplankton in southern California coastal waters."*

Although **Eppley *et al.*(1979)** might not get high marks in a philosophy of science or logic class, their paper is still a remarkable achievement for what they did accomplish. Pay close attention to the methods used in this paper. Many of these methods, being used in a large field survey for the first time, became models for a decade or more of field sampling programs. They used 24-h simulated *in situ* incubations to estimate primary productivity. This study clearly separated 'new' from regenerated production, concepts introduced by **Dugdale & Goering (1967)** (see Appendix-1 for definitions). To do this, the authors used the stable isotope of nitrogen ^{15}N to measure NO_3^- and NH_4^+ uptake. The authors used biological uptake rates of nitrate, and observed nitrate gradients to estimate vertical eddy diffusivities.

When reading this paper, don't skip over the line on page 484:

> *"On the other hand, elemental carbon:nitrogen ratios of particulate matter in the photic zone are in the range of 4-9 by atoms, as in N-limited continuous cultures of phytoplankton maintained at near maximum growth rates. The phytoplankton are rich in nitrogen compared to those in N-limited continuous cultures operated at low growth (dilution) rates (Caperon & Meyer 1972)."*

This paper appeared at just about the same time as **Goldman *et al.*'s (1979)** paper, which argued that phytoplankton in the ocean are growing at high relative growth rates or the C:N ratios would be much higher than the Redfield expectation of 6.

Outline of Papers

REQUIRED

Eppley, R. W., E. H. Renger, and W. G. Harrison. 1979. Nitrate and phytoplankton production in southern California coastal waters. Limnol. Oceanogr. *24*: 483-494

Abstract
- a. Transport of NO_3^- appears to be a major factor regulating standing stock and production
- b. Evidence:
  - i. Production is proportional to NO_3^- uptake
  - ii. Phytoplankton standing stock is related to the depth of the vertical nitrate concentration gradient
  - iii. The chemical composition of the POC matter (POC:PON ratio), is related to the C:N assimilation ratio of the phytoplankton
  - iv. Regenerated production proportional to nitrate assimilation rate, implying parallel and concurrent increases in the production of heterotrophic microplankton.
  - v. Vertical diffusion of nitrate matches eddy diffusivity.

2. Introduction
- a. Is nutrient input from depth the driving force for phytoplankton growth?
- b. Surface NO_3^- values < 0.5µM & a clear nitracline is present

c. Nitracline is only approximately correlated with vertical gradients of temperature and density. (deeper than density gradients)
d. Phytoplankton standing stock is inversely correlated with nitracline depth.
e. NO_3^- appears to be limiting
   i. NO_3^- spikes increases production
   ii. plots of P *vs*. N gives positive intercepts on the P axis
   iii. ambient concentrations far less than saturation point on Monod uptake curves
f. **On the other hand, elemental C:N ratios are in the range of 4-9 by atoms, as in N-limited continuous cultures of phytoplankton maintained at near-maximum growth rates. (p. 484, top right)**
g. Sets up a null hypothesis on p. 484 and tests it:
   "However, the null hypotheses that the input of nitrate is independent of phytoplankton production may be tested in several ways, some of which have already been implied.
h. New vs regenerated production.
   i. New:total proportional to primary production rates.
      (1) Gyres: 100-150 mg C/m^2/d, ratio is 0.1
      (2) Upwelling: >2 g C/m^2/d, ratio >0.8
      (3) S. California: 500 mg to 1 g C/m^2/d, ratio is 0.3 to 0.4

i. 3 subordinate null hypotheses: [straw men] p. 485
   i. no relation between C and nitrate assimilation rates (i.e., the system runs on ammonium or other N sources, *e.g.*, coastal effluent)
   ii. temporal and spatial patterns of Nitrate input rate are independent of phytoplankton production rates
   iii. calculations of diffusive nitrate flux based on nitrate concentrations gradients and assimilation rates will give unreasonable estimates of primary production

3. **Methods**
   a. 11 quarterly 1977 cruises
   b. Biology Secchi depth, in situ chl fluorescence, simulated in situ 90, 30, 10, 5, 1, and 0.5% light depths
   c. Nutrients, CHN analysis
   d. chl a by fluorometry
   e. phytoplankton carbon measured from POC
   f. ^{14}C 24 h incubations on deck
   g. 0.1 µM spike of ^{15}N-NO_3^- or ^{15}N-ammonium, incubated for 24 hours
4. **Results**
   a. Relation between carbon and nitrate assimilation rates
      i. Figure 2 used to reject A.

Fig. 2. Relationship between primary production as carbon vs new production expressed as nitrate assimilation rate.

Fig. 3. Primary production in southern California vs. ratio $\frac{NO_3^{-1}\ assimilation}{NO_3^{-1} + ammonium\ \ assimilation}$

   ii. High levels of nitrate flux are a necessary but not sufficient condition for predicting primary production
   b. Relation between carbon and nitrogen assimilation and the composition of the particulate matter

Fig. 4. Plot of carbon:nitrogen assimilation vs POC:PON ratio, slope of 1.98. Since urea was 28% of total N assimilation and was not measured the expected slope would be 1/(1-.28)=1.39

   c. Relation between new and regenerated production

Fig. 5 Relation between ammonium and nitrate assimilation

   d. Rates of nitrate input to the euphotic zone.

Fig. 6. NO_3^- concentration vs σ_t.

$$\frac{dN}{dt} = 0 = -\rho\ NO_3^- + \frac{\partial}{\partial x}\left(K_z \frac{\partial N}{\partial z}\right). \qquad (1)$$

- Horizontal eddy diffusion might account for 10% to 100% of the nitrate required (bottom left, p. 489)

e. Vertical diffusion of nitrate
   i. What eddy diffusivities would be required to maintain the observed assimilation rates and nitrate gradients?
   ii. Upwelling observed at one station. Predicted Upwelling rates of 2.1 m d^{-1} was close to the natural range 1-10 m d^{-1}.

f. Relations between nitrate and phytoplankton standing stocks.
   i. z_n is the depth to the 1μM NO_3^- concentration. It is inversely related to primary production and phytoplankton standing stock.

$$\mu P\left(\frac{production}{m^2}\right) = F = K_z\left(\frac{dN}{dz}\right). \quad (5)$$

$$\mu P\left(\frac{production}{m^3}\right) \approx \frac{K_z\left(\frac{dN}{dz}\right)}{z}. \quad (6)$$

   ii. computed K_z values are reasonable: 2.7 m^2/d

g. Strong correlation between K_z and primary production

5. **Discussion**
   a. Relation between primary production and NO_3^- assimilation.
      i. reject H_o one and two
      ii. Ammonia from waste plants counts as new production near Santa Monica Bay. F ratios of 0.1 and PP of 2-3 g $C/M^2/d$
   b. Nitrate transport
      - eddy diffusivities reasonable, reject 3rd null hypothesis
   c. New vs. regenerated production
   d. Implications
      i. Lasker's stable-ocean hypothesis.
      ii. Measurement of New: Total production may provide an independent measure of sinking losses from the euphotic zone.

6. All 3 subordinate null hypotheses rejected.

Riley, G. A. 1967. Mathematical model of nutrient conditions in coastal waters. Bull. Bingham Oceanogr. Coll. *19*: 72-80.

1. Abstract:
   a. A mathematical model is developed to illustrate the distribution of nitrate and phosphate in coastal waters.
   b. The model depends on a deep-water source of nutrients at the edge of the continental shelf
   c. The model determines the nutrient distribution in relation to vertical mixing and biological rates of regeneration and utilization.
2. Introduction:
   a. Coastal waters are more productive than the open ocean & two factors responsible
      i. shore-ward transport from edge of continental shelf
      ii. enrichment by freshwater drainage [& anthropogenic influences]
   b. Salt balance from Cape Cod to Chesapeake Bay indicates little freshwater input and that input has relatively low nutrients relative to offshore waters.
   c. Annual production of 160 g C/m^2 inshore to 135 g C/m^2 offshore Ryther & Yentsch (1958)
   d. Water at edge of shelf contains 15 to 24 μg-atm NO_3^--N/l and 1.0 to 1.5 μg-at P/l with an N:P ratio of 15:1.
      - N is limiting
   e. A simple model will be proposed.

3. The physical model:
   a. 25-km stations
      - equations in finite-difference form
   b. 2-layer system
      - Mixing uniform within layers
   c. Vertical mixing
      i. 10% d^{-1} at station 1
      ii. 5% d^{-1} at station 2
      iii. 2% d^{-1} at station 3
      iv. and 1% d^{-1} at the remaining stations.
   d. Horizontal eddy diffusion
      i. Horizontal eddy diffusion, observed = 0.58 - 4.96 x 10^6 cm^2/sec
      ii. 2% horizontal exchange per day is equivalent to an eddy diffusion of 2.9 x 10^6 cm^2/sec, which is near the mean of computed values.

$$\frac{\partial N}{\partial t} = R + \frac{\partial}{\partial x}\left(\frac{A_x}{\rho}\frac{\partial N}{\partial x}\right) + \frac{\partial}{\partial z}\left(\frac{A_z}{\rho}\frac{\partial N}{\partial z}\right).$$

$$\begin{aligned} \textit{where, } A_x &= \textit{dynamic horizontal eddy diffusivity.} \\ A_z &= \textit{dynamic vertical eddy diffusivity.} \\ \frac{\partial}{\partial x} &= \textit{first derivative in x-direction.} \\ \frac{\partial}{\partial z} &= \textit{first derivative in z-direction.} \\ R &= \textit{Biological rate of change.} \end{aligned} \qquad (1)$$

Stations spread out from 1 to 25 to 50 to 75 to 100 to 125 km (6 blocks)

At Station 2:

$$\frac{\partial N_2}{\partial t} = R + 0.02N_1 + 0.02N_3 + 0.05N_2' - 0.09N_2. \qquad (2)$$

   e. Assumptions:
      i. the whole system is in steady state
      ii. the whole system is controlled by nutrient concentration
      iii. utilization = 10% of concentration, *e.g.*, in Box 2:
      $R = -0.10N_2$

Station 2 N_2 & N_2':

$$\begin{aligned} \frac{\partial N_2}{\partial t} &= 0.02N_1 + 0.02N_3 + 0.05N_2' - 0.09N_2 - 0.10N_2 = 0 \\ &= 0.02N_1 + 0.02N_3 + 0.05N_2' - 0.19N_2 = 0 \\ \frac{\partial N_2'}{\partial t} &= 0.02N_1' + 0.02N_3' + 0.05N_2 + 0.10N_2 - 0.09N_2' = 0 \\ &= 0.02N_1' + 0.02N_3' + 0.15N_2 - 0.09N_2' = 0 \end{aligned} \qquad \textbf{(11)}$$

   f. A final simultaneous solution is calculated. *[Such a solution can be calculated using eigenanalysis.]*

4. **Calculated results.**
   a. Figure 1. Nutrient gradients along a coastal water profile...**the families of curves show gradients that result when regeneration in the bottom layer is 50 to 100% of nutrient utilization in the surface layer.**
   "This kind of distribution is often seen in coastal waters, and suggests that the distribution is due in whole or in part to enrichment by drainage, but the model shows that an offshore nutrient source plus increased vertical mixing near shore will provide a satisfactory explanation".(bottom of p. 76)
   b. Figure 1 shows what happens when nutrient regeneration varies between 50 and 100% of surface utilization [the rest would go to sediments]
   c. Nitrogen concentrations are low in New England surface waters in summer, suggesting an 80% regeneration rate [probably lower than that]
   d. **A second model**
      i. Assumptions
         (1) N regeneration is 80%
         (2) Source at shelf is 15 µM
         (3) Deep-water P is 1µM
         (4) N:P utilization is 15:1
         (5) P regeneration is 100%
      ii. Results of 2nd model
         (1) **Figure 2**. N:P ratio decrease to 2.2:1 nearshore
         (2) Surface: Bottom P ratio is 87%, but for N is 61%
5. Discussion
   a. little difference in nearshore-offshore production
   b. over a 6 mo growing season 25 µmoles/l removed to the sediments
   c. this would be regenerated in winter.
   d. A large quantity of the nutrients remain inshore at the time of the diatom flower in late winter or spring, leading to a higher level of production

SUPPLEMENTAL

Ryther, J. H. and W. M. Dunstan 1971. Nitrogen, phosphorus and eutrophication in the coastal environment. Science *171*: 1008-1013.

1. Abstract.
   a. distribution and bioassay
   b. 2 x phosphate present
   c. low N:P in human waste, P regenerates more quickly
   d. reduction of phosphate from detergents will not improve coastal eutrophication.
2. RKR ratios
   a. N:P may range from 3 to 30
   b. ratio varies according to algae and nutrient input
   c. 10:1 is close to average
3. N often reduced to undetectable levels
4. Nitrogen from ducks in Moriches Bay

Fig. 2 Ammonium enrichment experiments A known species was added
Fig. 5 DIN profiles away from the coast
Fig. 6. DIP profiles

5. *Skeletonema costatum* pulses.
6. Sources and mechanisms
   a. Primary effluent has N:P in ratios of 5.8:1, Secondary is 5.4:1
   b. mistake of using DIP as a tracer of sewage
7. **"Coastal waters already receive the sewage of roughly half the population of the United States. To replace a portion of the phosphate in this sewage with a nitrogenous compound [nitriloacetic acid=NTA] and to then discharge it into an environment in which eutrophication is nitrogen limited may be simply adding fuel to the fire."**

References

Adams, E. E., J. W. Hansen, R. L. Lago, P. Clayton, and X. Zhang. 1992. A simple box model of the Nitrogen cycle in Boston Harbor and the Massachusetts Bays. Civil Engineering Practice (Fall 1992): 91-103. *[The most recent published analysis of the effects of the MWRA outfall on Nitrogen cycling in MA Bay. The conclusion: with best case estimates, about 5% of the existing MWRA N loading is lost through denitrification in Boston Harbor sediments. Another 2.5% is lost through burial. About 25% of the nitrogen lost through denitrification comes from the Gulf of Maine or other MA Bay sources. Moving the outfall should result in only a 6% increase in nitrogen loading to MA Bay. Secondary treatment will reduce total N loading by 15%, resulting in a net 9% reduction in loading, about the same as occurred when sludge stopped being dumped in the harbor in December 1991]*

Blanton, J. O., J. A. Yoder, L. P. Atkinson, T. N. Lee, C. R. McClain, D. W. Menzel, G. A Paffenhöfer, L. J. Pietrafesa, L. R. Pomeroy, and H. L. Windom. 1984. A multidisciplinary oceanography program on the southeastern U.S. continental shelf. EOS (12/4/84): 1202-1203. *[The physical, chemical and biological oceanography of the shelf is briefly introduced. Seasonal changes in the physical regime transport inner shelf material to the outer shelf where it may be entrained into the Gulf stream.]*

Boicourt, W. S., S-Y. Chao, H. W. Ducklow, P. M. Glibert, T. C. Malone, M. R. Roman, L. P. Sanford, J. A. Fuhrman, C. Garside, and R. W. Garvine. 1987. Physics and microbial ecology of a bouyant estuarine plume on the continental shelf. Eos *68*: 666 (Aug. 4 edition). *[The results of the interdisciplinary MECCAS program are summarized.]*

Dugdale, R. C. and J. J. Goering. 1967. Uptake of new and regenerated forms of nitrogen in primary productivity. Limnol. Oceanogr. *12*: 196-206. *[The terms new and regenerated production were coined in this paper. New production is production coupled to recently introduced nitrogen in a system, usually the production coupled to NO_3^- as the nitrogen source, but can include other sources of 'new' nitrogen such as urea from sewer outfalls. Regenerated production is primary production using nitrogen that has already been used once or more by phytoplankton cells within the euphotic zone]*

Eppley, R. W., A. F. Carlucci, O. Holm-Hansen, D. Kiefer, J. J. McCarthy, E. Venrick and P. M. Williams. 1971. Phytoplankton growth and composition in shipboard cultures supplied with nitrate, ammonium, or urea as the nitrogen source. Limnol. Oceanogr. *16*: 741-751.

Eppley, R. W., W. G. Harrison, S. W. Chisholm, and E. Stewart. 1977. Particulate organic matter in surface waters off Southern California and its relationship to phytoplankton. J. Mar. Res. *35*: 671-695.

Falkowski, P. G., J. Vidal, T. S. Hopkins, G. T. Rowe, T. E. Whitledge, and W. G. Harrison. 1984. Summer nutrient dynamics in the middle Atlantic Bight: primary production and utilization of phytoplankton carbon. J. Plankt. Res. *5*: 515-537.

Goldman, J. C. 1980. Physiological processes, nutrient availability, and the concept of relative growth rate in marine phytoplankton ecology. Pp. 179-194 *in* P. G. Falkowski, ed, Primary Productivity in the Sea. Plenum Press, New York. *[Phytoplankton only have RKR ratios when μ/μ_m is roughly 1. DiTullio now has a rapid method for estimating relative growth based on ^{14}C activity in protein.]*

Goldman, J. C., J. J. McCarthy, and D. G. Peavey. 1979. Growth rate influence on the chemical composition of phytoplankton in oceanic waters. Nature *279*: 210-215. *[A very important paper! The C:N and C:P ratios from chemostat studies are reviewed and it is shown that phytoplankton only grow with Redfield ratios at high relative growth rates 0.9 < μ/μ_{max} < 1. They introduce the controversial hypothesis that patches of nutrients from zooplankton excretion explain high relative growth rates in the field]*

Gross, M. G. (editor) 1975. The middle Atlantic continental shelf and New York Bight. ASLO Special Symposium publication.

Harris, G. P. 1986. Phytoplankton ecology. Chapman and Hall.

Mann, K. H. and J. R. N. Lazier. 1991. Dynamics of marine ecosystems: biological-physical interactions in the oceans. Blackwell Scientific Publications. *[Includes a nice introduction to the interplay of physical and biological processes. Chapter 6 on coastal fronts is superb.]*

Mills, E. L. 1989. Biological Oceanography: An early history. Cornell University Press, Ithaca NY and London.

Perry, R. I., B. R. Dilke, and T. R. Parsons. 1983. Tidal mixing and summer plankton distributions in Hecate Strait, British Columbia. Can. J. Fish. Aquat. Sci. *40*: 871-887. *[Ian Perry tests Pingree's North Sea water-column stability model for BC coastal waters. It works.]*

Pingree, R. D. 1978. Mixing and stabilization of phytoplankton distributions on the northwest European continental shelf. Pp. 181-220 *in* J. H. Steele, ed., Spatial patters in plankton communities, Plenum Press. *[Pingree introduces a scaling parameter to assess the degree of water-column stability in coastal waters. This model appears to fit North Sea (Pingree), British Columbia (I. Perry) and Long Island Sound phytoplankton (Bowman et al. 1981).]*

Pingree, R. D., P. M. Holligan, and G. T. Mardell. 1978. The effects of vertical stability on phytoplankton distributions in the summer on the northwest European shelf. Deep-Sea Res. *25*: 1011-1028.

Pomeroy, L. R., G.-A. Paffenhöfer, and J. A. Yoder. 1987. Interaction of phytoplankton, zooplankton and macroorganisms. Prog. Oceanogr. *19*: 353-372.

Ryther, J. H. and W. M. Dunstan 1971. Nitrogen, phosphorous and eutrophication in the coastal environment. Science *171*: 1008-1013. *[R & D. describe a series of cruises in the New York bight designed to show that nitrogen, not phosphorous, is the limiting nutrient to marine phytoplankton.]*

Sverdrup, H. U. 1953. On conditions for the vernal blooming of phytoplankton. J. Conseil perm. int. Explor. Mer. *18*: 287-295.

Takahashi, M., D. L. Seibert, and W. H. Thomas. 1977. Occasional blooms of phytoplankton during summer in Saanich Inlet, B. C., Canada. Deep-Sea Research *24*: 775-780.

Townsend, D. W. and R. W. Spinrad. 1986. Early phytoplankton blooms in the Gulf of Maine. Cont. Shelf Res. *6*: 515-529. *[Sverdrup's critical-depth concept is applied to the Gulf of Maine. If the light attenuation coefficient is known, and an average compensation light intensity for the water column is assumed (40 langley's per day), then the onset of the spring bloom can be predicted. Spring blooms in Ma Bay appear later than Townsend and Spinrad's model would predict.]*

Wofsy, S. C. 1983. A simple model to predict extinction coefficients and phytoplankton biomass in eutrophic waters. Limnol. Oceanogr. 28: 1144-1155. *[The optical depth of the mixed layer in nutrient-rich systems is between 5 and 10. Phytoplankton, within 15 days, will increase in standing stock until the populations are light limited. Phytoplankton standing crops and production can be predicted if the light absorbed by nonliving material is known. To estimate the potential effects of eutrophication, one needs to know: 1) mixing depth, 2) total light extinction, and 3) extinction due to nonliving and refractory materials. Wofsy applies his equations to the analysis of nutrient enrichment in aquatic systems]*

Yoder, J. A. 1985. Environmental control of phytoplankton production on the Southeastern U. S. Continental Shelf. Pp. 93-103 *in* Oceanography of the Southeastern U. S. Cont. Shelf, Coastal and Estuarine Sciences 2. AGU.

On Markov modeling

Eisenfeld, J. 1979. Relationship between stochastic and differential models of compartmental systems. Math. Biosci. *43*: 282-305. *[This wonderful little paper shows you how to convert 1st order differential equation box models to Markov models. Note that the rows to columns convention has been transposed here. Eisenfeld uses from columns to rows. The matrix exponential function is available in Matlab as expm.m]*

Kemeny, J. G. and J. L. Snell. 1976. Finite Markov chains. Springer-Verlag, New York, New York, U.S.A. *[An earlier edition of this book is available in the UMASS/Boston library.]*

Moler, C. 199 1993? dubious ways to compute the matrix exponential. SIAM Reviews.

Roberts, F. S. 1976. Discrete mathematical models with applications to social, biological, and environmental problems. Prentice-Hall, Englewood Cliffs, New Jersey.

Is Fe limiting production in the Southern California Bight?

Bruland, K. W., E. L. Rue, and G. J. Smith. 2001. Iron and macronutrients in California upwelling regimes: implications for diatom blooms. Limnol. Oceanogr. *46*: 1661-1674 *[Monterey Bay and north is Fe-replete, and large diatom blooms result. South of Monterey, in the Big Sur regions, Fe is depleted (< 1 nM), indicative of HNLC systems. See also **Hutchins & Bruland 1998**]* {**35**}

Hutchins, D. A. and K. W. Bruland 1998. Iron-limited diatom growth and Si:N uptake ratios in a coastal upwelling regime. Nature 393: 561-564. *[Commentary by **Boyle 1998**. Evidence for Fe limitation in the Big Sur region. Diatoms stressed by lack of iron deplete surface waters of silicic acid. Fe limitation leads to faster sinking diatoms See also **Bruland et al. 2001.**]* {**3**, **35**}

Hutchins, D. A., G. R. DiTullio, Y. Zhang, and K. W. Bruland. 1998. An iron limitation mosaic in the California upwelling regime. Limnol. Oceanogr. *43*: 1037-1054. *[4 Fe addition experiments described with indications of strong Fe limitation of production south of Monterey Bay]{?}*

Miscellaneous

Altabet, M. 1989. A time-series study of the vertical structure of nitrogen and particle dynamics in the Sargasso Sea. Limnol. Oceanogr. *34*: 1185-1201.

Brandt, K. 1899. Ueber den Stoffwechsel im Meere. Rede beim Antritt des Rektorates der Königlichen Christian-Albrechts-Universität zu Kiel am 6. März 1899. Kiel: Universitäts-Buchandlung. 36 pp. *[Brandt introduces his denitrification hypothesis: 'denitrifying bacteria in the ocean remove the excess of nitrogen compounds and that it is they that restore the prevailing equilibrium of nature's household.' Quoted in **Mills 1989**, p. 51]*

King, F. D. and A. H. Devol. 1979. Estimates of vertical eddy diffusion through the thermocline from phytoplankton nitrate uptake rates in the mixed layer of the eastern tropical Pacific. Limnol. Oceanogr. *24*: 645-651. *[^{15}N-NO_3^- uptake is combined with vertical NO_3^- gradients to calculate K_z's through the thermocline. The approach, similar to Eppley et al. 1979, produces K_z's of .05-1.1 cm^2s^{-1}. A log-log relationship between $d\sigma_t/dz$ and K_z is used to predict NO_3^- flux. An indirect estimate of the f ratio is produced ranging from 4.3 to 75.3%]*

Lewis, M. R., W. G. Harrison, N. S. Oakey, D. Herbert and T. Platt. 1986. Vertical nitrate fluxes in the oligotrophic ocean. Science *234*: 870-873. *[They estimated K_z using turbulent kinetic energy fluctuations, the N gradients, and ^{15}N uptake. They calculate low rates of new production (.14 mmol $Nm^{-2}d^{-1} \approx 1$ mmol C $m^{-2}d^{-1}$). This is in accord with "older" estimates of gyre production. The vertical nitrate flux is not sufficient to account for the newly proposed high gyre production rates.]*

Tremblay, J.É., B. Klein, L. Legendre, R. B. Rivkin, and J-C. Therriault. 1997. Estimation of *f*-ratios in oceans based on phytoplankton size structure. Limnol. Oceanogr. *41*: 595-601 *[f-ratis are linear fractions of size-fractionated production and biomass.]*

Index